

Unbiased Rotational Moves for Rigid-Body Dynamics

Daniel A. Beard* and Tamar Schlick†

*Department of Bioengineering, University of Washington, Seattle, Washington; and †Department of Chemistry, Courant Institute of Mathematical Sciences, and Howard Hughes Medical Institute, New York University, New York, New York

ABSTRACT We introduce an unbiased protocol for performing rotational moves in rigid-body dynamics simulations. This approach—based on the analytic solution for the rotational equations of motion for an orthogonal coordinate system at constant angular velocity—removes deficiencies that have been largely ignored in Brownian dynamics simulations, namely errors for finite rotations that result from applying the noncommuting rotational matrices in an arbitrary order. Our algorithm should thus replace standard approaches to rotate local coordinate frames in Langevin and Brownian dynamics simulations.

INTRODUCTION

Generalized numerical methods for Langevin or Brownian dynamics (BD) involving rigid bodies require operators for applying arbitrary finite rotational moves to three-dimensional objects. Typically, a local body-fixed coordinate frame, which defines a body's three-dimensional orientation, is associated with each body in a system (García de la Torre and Bloomfield, 1981; Allison, 1991; Fernandez and García de la Torre, 2002). Such methods are important and commonly used to study large biomolecular systems, such as long DNA (Wu et al., 1991; Chirico and Langowski, 1996; Jian et al., 1997; Klenin et al., 1998) or large nucleoprotein complexes (Beard and Schlick, 2001; Huang and Schlick, 2002). During every time-step, each body is translated and rotated according to a given discretization of the governing dynamical equations (Ermak and McCammon, 1978; Allison, 1991; Fernandez and García de la Torre, 2002). The translational step is straightforward; it involves updating the three coordinates of a body's center of rotation. The rotational step is more subtle, because operators for rotation about orthogonal axes do not commute and thus their order of application defines different protocols. The related difficulties have been ignored in the past (e.g., Allison, 1991; Fernandez and García de la Torre, 2002); that is, the noncommuting operators are usually applied in some particular (arbitrary) order, introducing errors and bias into the rotational move. Although most prior models with BD simulation protocols have been assessed relative to available experimental data and found to be satisfactory overall, the previously-used rotational operators are strictly appropriate only in the limit of small rotational angles, where these errors are negligible. Here we address this limitation by exploring the magnitudes of angles for which errors become apparent in a simple model and introduce an unbiased accurate operator for finite rotations. Given that our protocol has the same computational cost as the biased protocol, it should be

used in general in BD algorithms to avoid any possible errors from this computational component.

ROTATIONAL MOVES

We define a right-handed local particle-fixed coordinate frame for a rigid body using three orthogonal unit vectors $\{\hat{a}, \hat{b}, \hat{c}\}$, which translate and rotate in space as a dynamics trajectory evolves (e.g., Fig. 1 of Beard and Schlick, 2001). In this article, we focus on how a given rotation is applied to a coordinate frame; we do not consider issues related to how the dynamical equations are discretized to determine the rotation and translation vectors for each time-step.

A finite rotation is denoted by $\vec{\Omega} = \{\Omega_a, \Omega_b, \Omega_c\}$, where the components of $\vec{\Omega}$ are rotations about the three orthogonal local axes. The central problem is posed as follows. Given a rotation vector $\vec{\Omega}$, how can this rotation be applied to a coordinate frame $\{\hat{a}, \hat{b}, \hat{c}\}$? This issue is key in simulating Brownian dynamics of rigid bodies (Allison, 1991; Fernandez and García de la Torre, 2002). In previous works, a three-dimensional rotation is applied to a coordinate frame by successively applying individual rotations about each local frame. In this approach, the successive rotation operators are given by

$$\begin{aligned} \mathbf{R}_a &= \begin{bmatrix} 1 & 0 & 0 \\ 0 & \cos \Omega_a & -\sin \Omega_a \\ 0 & \sin \Omega_a & \cos \Omega_a \end{bmatrix}, \\ \mathbf{R}_b &= \begin{bmatrix} \cos \Omega_b & 0 & \sin \Omega_b \\ 0 & 1 & 0 \\ -\sin \Omega_b & 0 & \cos \Omega_b \end{bmatrix}, \\ \mathbf{R}_c &= \begin{bmatrix} \cos \Omega_c & -\sin \Omega_c & 0 \\ \sin \Omega_c & \cos \Omega_c & 0 \\ 0 & 0 & 1 \end{bmatrix}, \end{aligned} \quad (1)$$

and the cumulative rotational operator \mathbf{R} is defined by applying these rotations in a particular order. For example, applying rotations about the \hat{a}, \hat{b} , then \hat{c} axes, yields

$$\mathbf{R} = \mathbf{R}_c \mathbf{R}_b \mathbf{R}_a. \quad (2)$$

Submitted May 19, 2003, and accepted for publication July 30, 2003.

Address reprint requests to Tamar Schlick, Courant Institute of Mathematical Sciences, New York University, 251 Mercer St., New York, NY 10012. Tel.: 212-998-3116; Fax: 212-995-4152; E-mail: schlick@nyu.edu.

© 2003 by the Biophysical Society

0006-3495/03/11/2973/04 \$2.00

However, this choice of \mathbf{R} is not unique. The rotation operators do not commute: $\mathbf{R}_a \mathbf{R}_b \mathbf{R}_c \neq \mathbf{R}_c \mathbf{R}_b \mathbf{R}_a$. Thus, the operator \mathbf{R} introduces bias into the coordinate rotation. As we show below for a given random rotation vector chosen from an unbiased distribution, resulting rotations will be biased toward an axis which is determined by the choice of the order of operators applied in Eq. 2.

BIAS-FREE ROTATIONAL APPROACH

A bias-free approach to performing these rotational steps can be formulated from the dynamics equations for rotation of an orthogonal coordinate system at a constant angular velocity (see Eq. 4-62 of Goldstein et al., 2002):

$$\begin{aligned}\frac{d\hat{a}}{dt} &= \omega_c \hat{b} - \omega_b \hat{c} \\ \frac{d\hat{b}}{dt} &= \omega_a \hat{c} - \omega_c \hat{a} \\ \frac{d\hat{c}}{dt} &= \omega_b \hat{a} - \omega_a \hat{b},\end{aligned}\quad (3)$$

where $\{\omega_a, \omega_b, \omega_c\}$ are the three components of angular velocity. For constant $\omega_a, \omega_b, \omega_c$, Eq. 3 is a constant-coefficient linear system with solution (which was obtained using the program MAPLE, Waterloo Maple, Waterloo, Ontario, Canada):

$$\begin{aligned}\hat{a}(t + \Delta t) &= \left[\frac{(\Omega_b^2 + \Omega_c^2) \cos \Omega + \Omega_a^2}{\Omega^2} \right] \hat{a}(t) + \left[\frac{\Omega_a \Omega_b}{\Omega^2} (1 - \cos \Omega) + \frac{\Omega_c}{\Omega} \sin \Omega \right] \hat{b}(t) + \left[\frac{\Omega_a \Omega_c}{\Omega^2} (1 - \cos \Omega) - \frac{\Omega_b}{\Omega} \sin \Omega \right] \hat{c}(t) \\ \hat{b}(t + \Delta t) &= \left[\frac{\Omega_a \Omega_b}{\Omega^2} (1 - \cos \Omega) - \frac{\Omega_c}{\Omega} \sin \Omega \right] \hat{a}(t) + \left[\frac{(\Omega_a^2 + \Omega_c^2) \cos \Omega + \Omega_b^2}{\Omega^2} \right] \hat{b}(t) + \left[\frac{\Omega_b \Omega_c}{\Omega^2} (1 - \cos \Omega) + \frac{\Omega_a}{\Omega} \sin \Omega \right] \hat{c}(t) \\ \hat{c}(t + \Delta t) &= \left[\frac{\Omega_a \Omega_c}{\Omega^2} (1 - \cos \Omega) + \frac{\Omega_b}{\Omega} \sin \Omega \right] \hat{a}(t) + \left[\frac{\Omega_b \Omega_c}{\Omega^2} (1 - \cos \Omega) - \frac{\Omega_a}{\Omega} \sin \Omega \right] \hat{b}(t) + \left[\frac{(\Omega_a^2 + \Omega_b^2) \cos \Omega + \Omega_c^2}{\Omega^2} \right] \hat{c}(t),\end{aligned}\quad (4)$$

where $\{\Omega_a, \Omega_b, \Omega_c\} = \{\omega_a \Delta t, \omega_b \Delta t, \omega_c \Delta t\}$, and $\Omega^2 = \Omega_a^2 + \Omega_b^2 + \Omega_c^2$.

Using the notation of Fernandez and García de la Torre (2002), Eq. 4 can be expressed compactly as

$$\begin{aligned}[\hat{a} \hat{b} \hat{c}] &= \\ [\hat{a}_0 \hat{b}_0 \hat{c}_0] &\times \begin{bmatrix} \left(\frac{(\Omega_b^2 + \Omega_c^2) \cos \Omega + \Omega_a^2}{\Omega^2} \right) & \left(\frac{\Omega_a \Omega_b}{\Omega^2} (1 - \cos \Omega) - \frac{\Omega_c}{\Omega} \sin \Omega \right) & \left(\frac{\Omega_a \Omega_c}{\Omega^2} (1 - \cos \Omega) + \frac{\Omega_b}{\Omega} \sin \Omega \right) \\ \left(\frac{\Omega_a \Omega_b}{\Omega^2} (1 - \cos \Omega) - \frac{\Omega_c}{\Omega} \sin \Omega \right) & \left(\frac{(\Omega_a^2 + \Omega_c^2) \cos \Omega + \Omega_b^2}{\Omega^2} \right) & \left(\frac{\Omega_b \Omega_c}{\Omega^2} (1 - \cos \Omega) - \frac{\Omega_a}{\Omega} \sin \Omega \right) \\ \left(\frac{\Omega_a \Omega_c}{\Omega^2} (1 - \cos \Omega) + \frac{\Omega_b}{\Omega} \sin \Omega \right) & \left(\frac{\Omega_b \Omega_c}{\Omega^2} (1 - \cos \Omega) - \frac{\Omega_a}{\Omega} \sin \Omega \right) & \left(\frac{(\Omega_a^2 + \Omega_b^2) \cos \Omega + \Omega_c^2}{\Omega^2} \right) \end{bmatrix},\end{aligned}\quad (5)$$

where the triad vectors $\{\hat{a}_0, \hat{b}_0, \hat{c}_0\}$ denote the initial local frame (at time t_0), and $\{\hat{a}, \hat{b}, \hat{c}\}$ correspond to the local axes following rotation (at time t). The matrix $\mathbf{M}^{t-t_0} = [\hat{a} \hat{b} \hat{c}]$ is a transformation from the local frame at time t to the fixed lab (l) frame. Thus Eq. 5 can be written $\mathbf{M}^{t-t_0} = \mathbf{M}^{t_0-t} \mathbf{U}$, where the matrix \mathbf{U} , defined by Eq. 5, replaces the operator \mathbf{R} in Eq. 2.

The matrix operator \mathbf{U} in Eq. 5 is an exact representation for the rotation of the vectors $\{\hat{a}_0, \hat{b}_0, \hat{c}_0\}$ by an angle Ω through the axis of rotation \hat{n} , where \hat{n} is the unit vector defined by $\hat{n} = \vec{\Omega}/\Omega$. Through geometric arguments, Goldstein et al. (2002) have shown that this rotation is expressed as

$$\vec{r} = \vec{r}_0 \cos \Omega + \hat{n}(\hat{n} \times \vec{r}_0)[1 - \cos \Omega] + (\hat{n} \times \vec{r}_0) \sin \Omega, \quad (6)$$

where \vec{r}_0 and \vec{r} represent a vector before and after rotation, respectively. Eq. 6—derived by rotating the frame to make the z -axis point along the axis of rotation, applying the rotation around this axis, and then rotating back—is equivalent to our matrix operation of Eq. 5.

EXAMPLE OF ROTATIONAL ERROR

To compare the performance of the above rotational operators, we consider the geometry illustrated in Fig. 1. Without loss of generality, we assume that the initial local

frame $\{\hat{a}_0, \hat{b}_0, \hat{c}_0\}$ coincides with the lab fixed coordinate system, indicated by the x -, y -, and z -axes. We consider rotations where $\vec{\Omega}$ is directed in the x - y plane. In particular, $\vec{\Omega} = \Omega[\cos \theta, \sin \theta, 0]^T$, where θ is the polar angle of $\vec{\Omega}$ (see Fig.

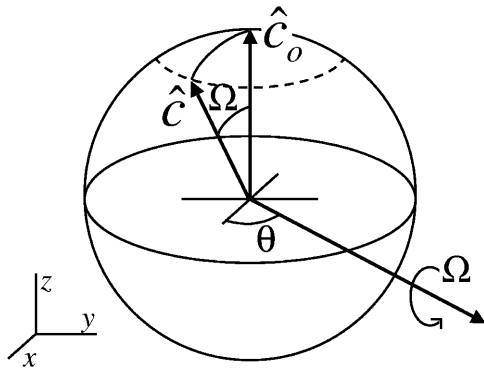


FIGURE 1 The unit sphere in the $\{x,y,z\}$ fixed lab frame. The initial local frame $\{\hat{a}_0, \hat{b}_0, \hat{c}_0\}$ corresponds to the fixed lab frame axes. The rotation vector $\hat{\Omega} = \Omega[\cos \theta, \sin \theta, 0]$ is oriented in the x - y plane; \hat{c} denotes \hat{c}_0 after being rotated about $\hat{\Omega}$.

1) and the superscript T denotes the vector transpose. The local frame following rotation is denoted by $\{\hat{a}, \hat{b}, \hat{c}\}$, with rotated \hat{c} component, $\hat{c} = [\sin \Omega \sin \theta, -\sin \Omega \cos \theta, \cos \Omega]^T$. The endpoint of \hat{c} , directed out of the origin, lies on a circle located in the plane at $z = \cos \Omega$. The transformation given by Eq. 5 produces the expected result, whereas the approximations $\mathbf{R}_c \mathbf{R}_b \mathbf{R}_a \hat{c}_0$ and the other variations are not exact, as we next show.

Specifically, we perform rotations on $\{\hat{a}_0, \hat{b}_0, \hat{c}_0\}$ at 18° intervals in θ for Ω of $10^\circ, 30^\circ,$ and 60° . In Fig. 2, we plot the resulting endpoints of \hat{c} for the six variations on the combinations of the noncommuting operators in \mathbf{R} . The x - and y -components of the rotated \hat{c} are plotted separately in Fig. 2; the three concentric circles in each plot correspond to the three different magnitudes of Ω . The solid circles correspond to the exact operator of Eq. 5; the unfilled circles correspond to the \mathbf{R} operators as indicated in each plot (*a-f*).

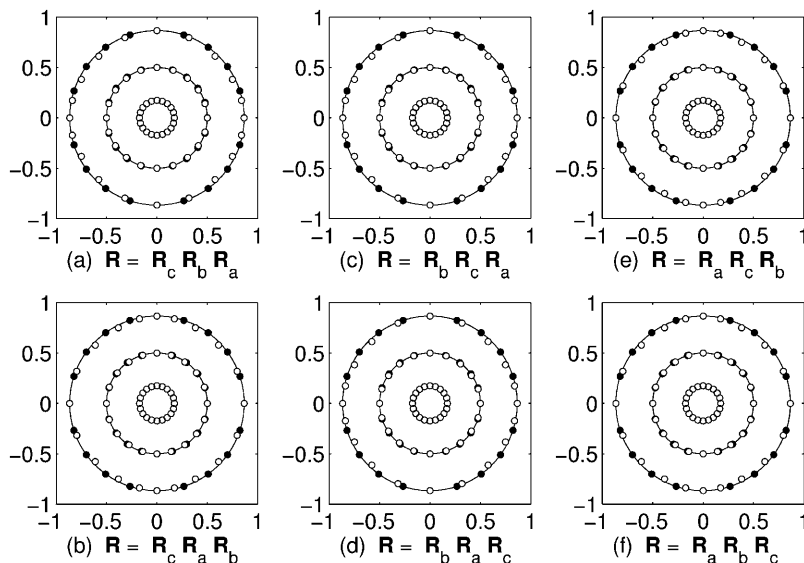


FIGURE 2 Positions of the x - and y -components of \hat{c} after rotating \hat{c}_0 by $\hat{\Omega}$. The initial local frame $\{\hat{a}_0, \hat{b}_0, \hat{c}_0\}$ corresponds to the lab fixed frame (see Fig. 1). Rotations are performed for 20 values of θ between 0° and 360° and Ω of $10^\circ, 30^\circ,$ and 60° . Solid circles correspond to the exact move; unfilled circles correspond to rotations by each of the six \mathbf{R} operators, as indicated in *a-f*. The \mathbf{R} operators depend on the definition used, with the bias and magnitude of error dependent on that choice of \mathbf{R} .

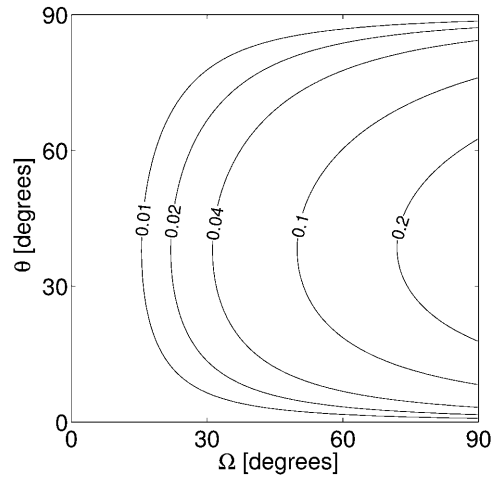


FIGURE 3 Contours of $E_c(\Omega, \theta) = \|\mathbf{R}\hat{c}_0 - \hat{c}\|/\|\hat{c}_0 - \hat{c}\|$ for the operator $\mathbf{R} = \mathbf{R}_c \mathbf{R}_b \mathbf{R}_a$ in the Ω - θ plane.

The behavior of the \mathbf{R} operator is clearly dependent on the definition used, with the magnitude of the error increasing with the size of the rotation, Ω .

To quantify the error associated with \mathbf{R} , we introduce a normalized error measure: $E_c(\Omega, \theta) = \|\mathbf{R}\hat{c}_0 - \hat{c}\|/\|\hat{c}_0 - \hat{c}\|$, which measures the magnitude in the error of the \mathbf{R} -rotated \hat{c} vector relative to magnitude of the exact move $\|\hat{c}_0 - \hat{c}\|$. Contours of $E_c(\Omega, \theta)$ for $\mathbf{R} = \mathbf{R}_c \mathbf{R}_b \mathbf{R}_a$ are plotted in Fig. 3. As expected, the relative error increases with Ω . The error goes to zero as the rotational angle goes to zero. For other definitions of \mathbf{R} , results are similar. This rotational operator is straightforward to implement in the standard Ermak and McCammon algorithm (Ermak and McCammon, 1978) and in higher-order BD updates, where repeated rotation applications may be necessary per time-step.

CONCLUSION

The commonly used rotation protocol for rigid-body dynamics introduces bias and error into the rotational move and hence the overall simulation. Here, we show that the bias and error are finite, yet diminish for small rotational angles. Our alternative rotational protocol (Eq. 5), applied to chromatin folding (Beard and Schlick, 2001), does not introduce additional numerical complexity and removes such biases and errors. It should thus be used to rotate local coordinate frames in rigid body dynamics.

The authors are grateful to Hong Qian for valuable discussions. They also thank Marshall Fixman and Bruce Robinson for comments on an alternative geometric approach.

REFERENCES

- Allison, S. A. 1991. A Brownian dynamics algorithm for arbitrary rigid bodies. Applications to polarized dynamic light scattering. *Macromolecules*. 24:530–536.
- Beard, D. A., and T. Schlick. 2001. Computational modeling predicts the structure and dynamics of chromatin fiber. *Structure*. 9:105–114.
- Chirico, G., and J. Langowski. 1996. Brownian dynamics simulations of supercoiled DNA with bent sequences. *Biophys. J.* 71:955–971.
- Fernandez, M. X., and J. García de la Torre. 2002. Brownian dynamics of rigid particles of arbitrary shape in external fields. *Biophys. J.* 83:3039–3048.
- García de la Torre, J., and V. A. Bloomfield. 1981. Hydrodynamic properties of complex, rigid, biological macromolecules. Theory and applications. *Q. Rev. Biophys.* 14:81–139.
- Ermak, D. L., and J. A. McCammon. 1978. Brownian dynamics with hydrodynamic interactions. *J. Chem. Phys.* 69:1352–1360.
- Goldstein, H., C. Poole, and J. Safko. 2002. *Classical Mechanics*, 3rd Ed. Addison-Wesley, San Francisco, CA. 134–183.
- Huang, J., and T. Schlick. 2002. Macroscopic modeling and simulations of supercoiled DNA with bound proteins. *J. Chem. Phys.* 117:8573–8586.
- Jian, H., A. Vologodskii, and T. Schlick. 1997. A combined wormlike-chain and bead model for dynamic simulations of long linear DNA. *J. Comp. Phys.* 136:168–179.
- Klenin, K., H. Merlitz, and J. Langowski. 1998. A Brownian dynamics program for the simulation of linear and circular DNA and other wormlike chain polyelectrolytes. *Biophys. J.* 74:780–788.
- Wu, P. G., B. S. Fujimoto, L. Song, and J. M. Schurr. 1991. Effect of ethidium on the torsion constants of linear and supercoiled DNAs. *Biophys. Chem.* 41:217–236.